Supporting Information For:

Spatially resolved ferroelectric domain-switching controlled magnetism in $Co_{40}Fe_{40}B_{20}/Pb(Mg_{1/3}Nb_{2/3})_{0.7}Ti_{0.3}O_3$ multiferroic heterostructure

Peisen Li,[1,2,3] Yonggang Zhao,[1,2] Sen Zhang,[1,2] Aitian Chen,[1,2] Dalai Li,[4] Jing Ma,[5] Yan Liu,[1,2] Daniel T. Pierce,[6] John Unguris,[6] Hong-Guang Piao,[7] Huiyun Zhang,[1] Meihong Zhu,[1] Xiaozhong Zhang,[7] Xiufeng Han,[4] Mengchun Pan[3] and Ce-Wen Nan[5]*

[1]Department of Physics and State Key Laboratory of Low-Dimensional Quantum Physics Tsinghua University, Beijing 100084, China

[2]Collaborative Innovation Center of Quantum Matter, Beijing 100084, China

[3]College of Mechatronics and Automation, National University of Defense Technology, Changsha 410073, China

[4]Beijing National Laboratory for Condensed Matter Physics, Chinese Academy of Sciences, Beijing 100190, China

[5]School of Materials Science and Engineering and State Key Lab of New Ceramics and Fine Processing, Tsinghua University, Beijing 100084, China

[6]Center for Nanoscale Science and Technology, National Institute of Standards and Technology, Gaithersburg, Maryland 20899, USA

[7]School of Materials Science and Engineering and Key Laboratory of Advanced Materials (MOE), Tsinghua University, Beijing 100084, China

E-mail: ygzhao@tsinghua.edu.cn

KEYWORDS: Electric-field control of magnetism, Ferroelectric domain switching, Spatially resolved, Scanning Kerr microscopy (SKM), SEMPA

S1. Sample preparation and experimental configuration

Figure S1a shows the schematic configuration of the CoFeB/PMN-PT (001) heterostructure with the sample edges (*x*, *y* and *z*) along the pseudo cubic [100], [010] and [001] directions of the PMN-PT crystal, respectively. The thickness of the amorphous CoFeB magnetic film is 20 nm. A 10 nm thick tantalum (Ta) was sputtered as a protection layer. Au layers with a 300 nm thickness were sputtered on both the top and bottom sides of the FM/FE heterostructure as the electrodes for M-E measurements, while for the MOKE and SEMPA measurements, the Au layer was only sputtered on the back side of the FE. The measurements of macroscopic magnetic properties were performed along the direction defined by the angle θ between the direction of the magnetic field (H) and the [100] crystal direction as shown in Figure S1a. For the M-E measurements, electric fields were applied by a voltage source with the positive electric field defined as pointing from the CoFeB to the PMN-PT.

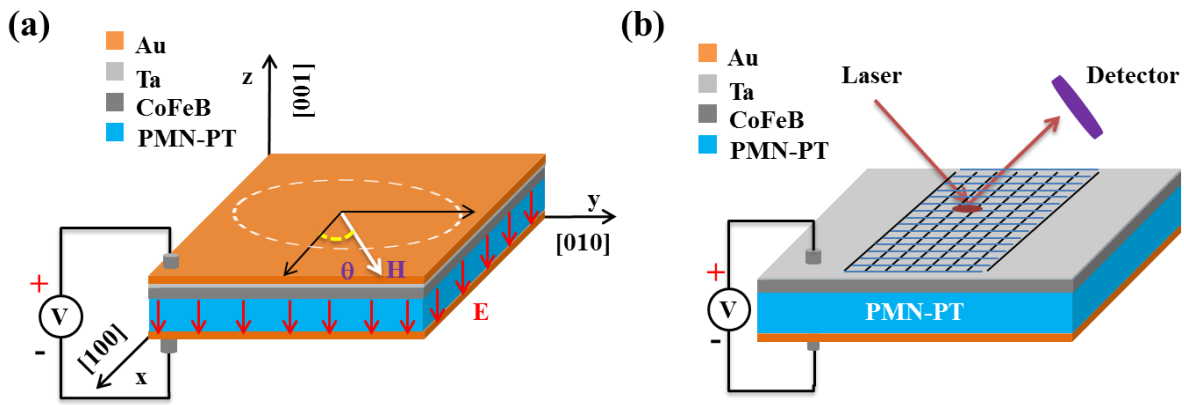

Figure S1. Sample configuration. Schematics of the sample configuration for in situ electric-field control of magnetism measured using (a) Superconducting quantum interference device (SQUID) and (b) MOKE and SKM.

The electrical modulation of the magnetic domains was measured via Scanning Kerr Microscopy (SKM) with an in situ electric field. As shown in Figure S1b, the electric fields were applied across the FM/FE heterostructure using a DC voltage source. During SKM mapping, the applied magnetic field was turned off, and the in-plane longitudinal

Kerr signal in each pixel was collected and reconstructed to get the magnetic moment maps as shown in Figure 2a. More details of the SKM setup and technique can be found in ref. 1.

S2. Ferroelectric properties of the PMN-PT ferroelectric single crystal

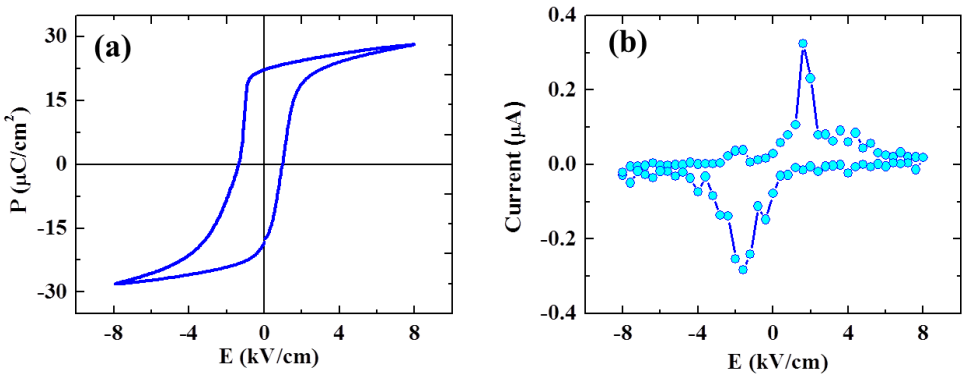

Figure S2. Ferroelectric properties of the PMN-PT (a) P-E loop for PMN-PT (001). The coercive field (E_c) of PMN-PT is about 1.5 kV cm^{-1}. (b) The polarization current of PMN-PT with a CoFeB top and an Au bottom electrode, demonstrating that the ferroelectric retains after the CoFeB deposition.

S3. Macroscopic characterization of the electric-field-controlled magnetism in the [-110] direction

Figure S3a shows the electric-field control of magnetization along the [-110] direction. The measurement was carried out with in situ electric fields and a 1 mT external magnetic field to define the measurement direction. The result exhibits a reverse behavior compared to that of the [110] direction (Figure 1a in the main text). The butterfly-like (M_B) and loop-like (M_L) M-E curves were separated from Figure S3a based on their symmetry with respect to the electric field polarity. Specifically, the butterfly component is described as $M_B(E) = \big(M(E) + M(-E)\big)/2 - \big(M(8) - M(-8)\big)/2$, which is symmetric with respect to the E = 0 axis. The loop component is written as $M_L(E) = \big(M(E) - M(-E)\big)/2 + \big(M(8) - M(-8)\big)/2$, which is antisymmetric with respect

to the E = 0 axis. $M(E)$ is the measured magnetization under the electric field (E) as shown in Figure S3a. Taking the state at E = –8 kV cm^{-1} as an example, the butterfly component is equal to $M_{\mathrm{B}}(-8)=\big(M(-8)+M(8)\big)/2-\big(M(8)-M(-8)\big)/2=M(-8)$ and the loop component is equal to $M_{\mathrm{L}}(-8)=\big(M(-8)-M(8)\big)/2+\big(M(8)-M(-8)\big)/2=0$. In this way, the two types M-E curves in the [-110] direction shown in Figure S3b were obtained.

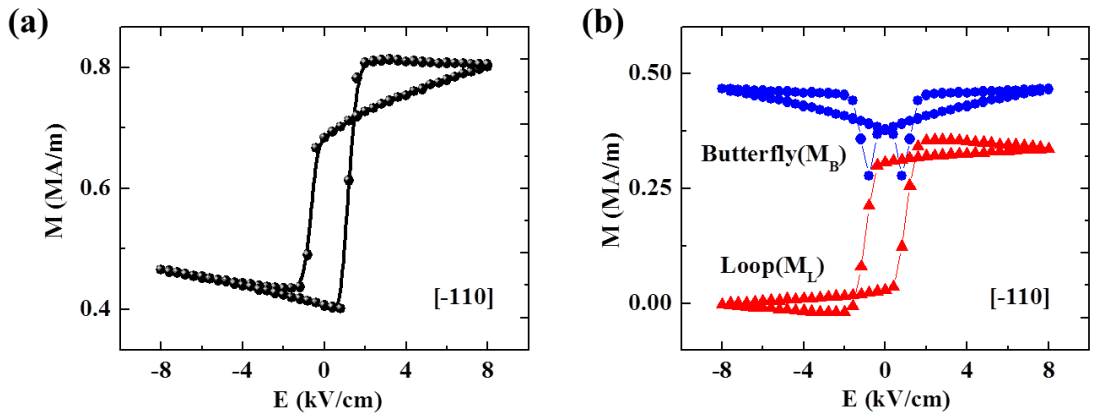

Figure S3. Magnetization of [-110] controlled by electric field. (a) M-E curves measured at 300 K along the [-110] direction with a 1 mT external magnetic field along [-110] direction. (b) The loop-like (red triangle) and butterfly-like (blue circle) M-E curves obtained from (a) based on their different responses to the polarity change of the electric field.

S4. Investigation of the electric-field control of the M-H curve along different crystal axes of PMN-PT

Figures S4a-c show the M-H hysteresis loops for the [-110], [110] and [100] crystal axes under ±4 kV cm^{-1}, respectively. The hysteresis loops demonstrate that the CoFeB has high remanence and is more easily magnetized in the [-110] direction when positive electric fields were applied as shown in Figure S4a. In contrast, negative electric fields make the magnetic film hard to magnetize in this direction. On the other hand, the effect of the electric field on the M-H hysteresis behavior for the [110] direction (Figure S4b) is reversed compared to that

of the [-110] direction. There is no obvious effect of the electric field on the M-H hysteresis curves for the [100] direction when ±4 kV cm^{-1} electric fields were applied as shown in Figure S4c. These results can be explained by the FE distortion changes due to the FE domain switching processes discussed in the main text and illustrated in Figure 4c. For example, the changes of strain in the [-110] and [110] directions are complementary due to the 109 ° switching, which leads to the complementary changes of M-H hysteresis for the [-110] and [110] directions (Figure S4a and Figure S4b). No distortion change occurs for the [100] direction whether the FE domain switching is 71 °, 109 ° or 180 ° as shown in Figure 4c, so no obvious change of M-H curve is seen for the [100] direction when ±4 kV cm^{-1} electric fields were applied (Figure S4c).

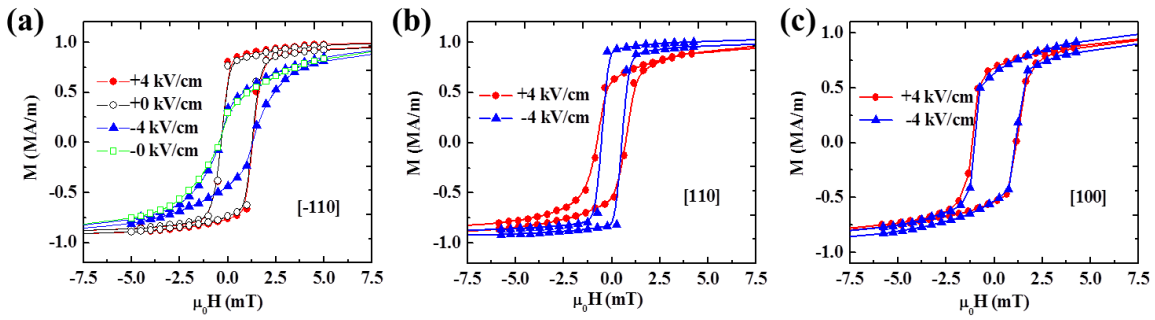

Figure S4. M-H hysteresis curves under different electric fields. (a-c) Magnetic hysteresis loops for the [-110], [110] and [100] directions under +4 kV cm^{-1} and -4 kV cm^{-1} electric field, respectively. M-H curves for the [-110] direction at E = 0 after +4 kV cm^{-1} and -4 kV cm^{-1} poling are also shown in (a), demonstrating the non-volatile nature of the electric-field-controlled magnetization.

S5. Electric-field-controlled magnetism characterized by the AC-mode MOKE technique

We used a lock-in technique to investigate the Kerr voltage response to a varying electric field with a frequency of 13 Hz (AC-mode MOKE). The details of this technique can be found in ref. 2. The results show that the M-E curve displays loop-like behavior in

some regions (Figure S5a), and butterfly-like behavior in other regions (Figure S5b). In our MOKE setup, we cannot apply a high AC voltage, so the maximum electric field used in AC MOKE measurement is lower than 1.5 kV cm^{-1}, which is only close to the E_c of the PMN-PT. In this case, the electric field used in the AC MOKE measurement is too weak to fully switch the FE domain, which leads to the difference between the AC MOKE curves (Figure S5) and results of macroscopic magnetization (Figure S3b), for which a 8 kV cm^{-1} electric field was reached.

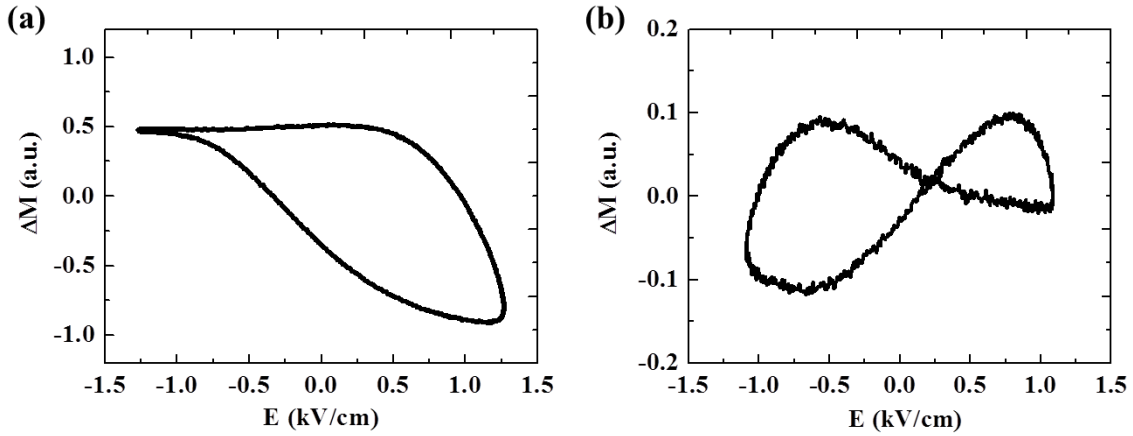

Figure S5. Local M-E curves measured by the AC-mode MOKE. (a) Loop-like M-E curve, (b) Butterfly-like M-E curve.

S6. Investigation of electric-field-controlled local magnetic anisotropy in different regions

We used the Rot-MOKE method[3] to investigate the local in-plane magnetic anisotropies of CoFeB under ±8 kV cm^{-1}, respectively, for the three typical regions as shown in Figure 2b. The results are shown in Figure S6. In regions 1 and 2 (loop-like), the magnetic free energy curves of the CoFeB film show that the anisotropies of CoFeB are uniaxial. The easy axes make angles with the [100] direction of θ = 102 ° and 111 ° under a positive electric field, in Figure S6a (region 1) and Figure S6b (region 2), respectively. So the easy axes in these two regions are far away from the [110] direction (θ = 45 °). On the other hand, after applying a negative electric field, the easy axes in these two regions rotate closer to the [110] direction (θ

= 62 °, 84 ° for regions 1 and 2, respectively), indicating a clear change in the anisotropies of regions 1 and 2 by electric fields. We note that the rotations of the easy axes in regions 1 and 2 are less than 90 °, perhaps due to the magnetic coupling with the magnetization in the adjacent regions. In contrast, there is no obvious difference between anisotropies associated with positive and negative electric fields in region 3 (butterfly-like), as shown in Figure S6c. Table S1 summarizes the numerical Rot-MOKE results for the electric field controlled local magnetic anisotropy.

Table S1 | The Rot-MOKE results for the local magnetic anisotropy

Point	(+8 kV cm^{-1})		(-8 kV cm^{-1})	
	H_k (mT)	θ (°)	H_k (mT)	θ (°)
1	**1.7**	**102**	**7.7**	**62**
2	**1.3**	**111**	**3.4**	**84**
3	**2.1**	**85**	**2.0**	**97**

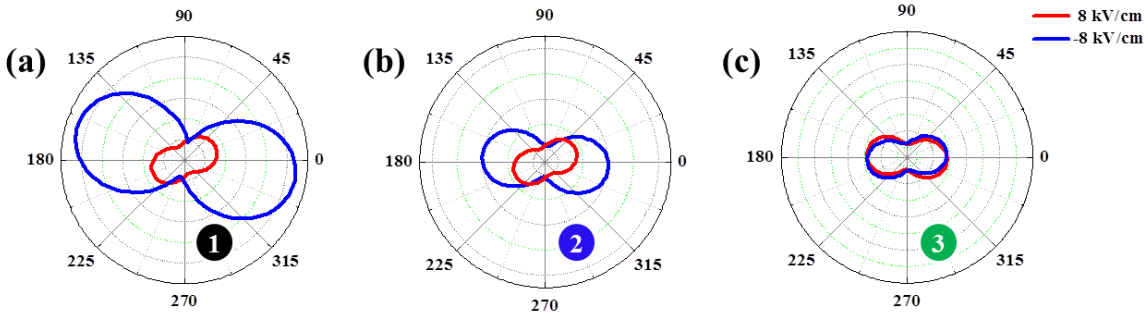

Figure S6. Electric-field control of local magnetic anisotropy. (a), (b) Regions 1 and 2. (c) Region 3. The free energy curves in red were measured after the positive electric field poling, while the curves in blue were measured after the negative electric field poling.

S7. Model for anisotropic modulation of the non-volatile electric-field control of magnetism

As discussed in the main text, the non-volatile electric-field control of magnetism originates from the 90 ° rotation of FM domains. After negative electric field poling, the

component of the FE polarization in the (001) plane of the sample surface is mostly along the [110]/[-1-10] axis. Most of the FM moments prefer to align along the in-plane FE polarization direction, i.e., along the [110]/[-1-10] axis. After positive electric field poling, some of the FE domains switch by 109 ° inducing a 90 ° rotation of the FM domain as previously reported.[4,5] Taking the FE domain with polarization along the [111] direction as an example, the positive electric field will switch the FE polarization 109 ° from [111] to [-11-1] or [111] to [1-1-1]. Figure S7 shows schematically a typical rotation process for one FM domain. The magnetic moment is approximately along the easy-axis because the applied magnetic field (1 mT) is lower than the local magnetoelastic anisotropic field (about 15 mT). This local magnetoelastic anisotropy field (H_σ) was obtained through $H_\sigma = 3\lambda \cdot Y \cdot S / M_s$, where S is the local strain induced by the FE rhombic distortion (0.2 % for PMN-PT),[4] Y is the Young's modulus (160 GPa for CoFeB), λ is the magnetostriction coefficient (2×10^{-5} for CoFeB),[6] and M_s is the saturation magnetization (1.2 MA m^{-1} for CoFeB). For positive electric field poling, the magnetization M_s prefers to stay along the [-110]/[1-10] direction and the measured magnetization M_+ can be expressed as $M_+ = M_s \cos(135° - \theta)$, where θ is the angle between H and the [100] direction. After negative electric field poling, M_s points in the [110] direction due to the 90 ° rotation of the FM domain. Thus, the measured magnetization M_- after the negative electric field poling can be written as $M_- = M_s \cos(45° - \theta)$. It should be mentioned that before the measurements of all the M-E curves, a 100 mT magnetic field was applied at θ to magnetize the sample, resulting in the angle between M_s and H smaller than 90 °. So the change of the measured M in magnitude between the positive electric field case and the negative electric field case, $M_+ - M_-$, for any θ can be written as $M_s\left|\cos(135° - \theta)\right| - M_s\left|\cos(45° - \theta)\right|$, i.e., $M_s\left(\left|\sin(\theta - 45°)\right| - \left|\cos(\theta - 45°)\right|\right)$.

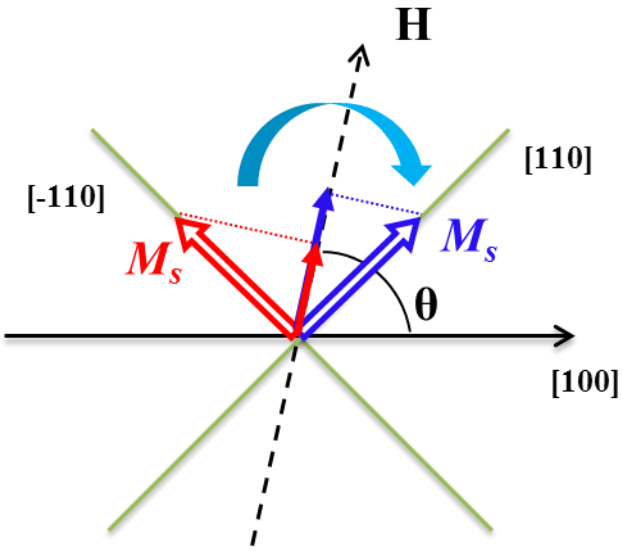

Figure S7. Model for anisotropic modulation. Illustration of the 90° rotation model and the anisotropy modulation of non-volatile electric-field control of magnetism. The measurement direction (*H*) deviates from the [100] direction by an angle θ.

However, because of the spatial inhomogeneity of the FE switching (and hence of the FM switching), not all of the domains in the [-110] direction switch to the [110] direction so the maximum change of $M_+ - M_-$ is less than M_s. To account for this, we assume that for positive electric field poling, the fraction of FM domains with magnetizations along the [-110] direction is P_1 and those along the [110] direction is $1-P_1$. After negative electric field poling, the fraction of FM domains with magnetizations along the [-110] direction is P_2 and those along the [110] direction is $1-P_2$. In this case, the net fraction of domains with magnetizations changed from the [-110] direction to the [110] direction is equal to P_1-P_2 as a result of 109° FE domain switching, and the net magnetization change is $(P_1-P_2)\cdot M_s$. Therefore, the angle-dependence of the non-volatile change in loop-like magnetization ΔM_L can be expressed as $(P_1-P_2)\cdot M_s\left(\left|\sin(\theta-45°)\right|-\left|\cos(\theta-45°)\right|\right)$. Let $\Delta M_{Max}=(P_1-P_2)\cdot M_s$; then $\Delta M_L=\Delta M_{Max}\left(\left|\sin(\theta-45°)\right|-\left|\cos(\theta-45°)\right|\right)$. This is used to fit the experimental data in Figure 1d with ΔM_{Max} as a fitting parameter.

References

(1) Gao, Y.; Hu, J.; Wu, L.; Nan, C.W. Dynamic In Situ Visualization of Voltage-Driven Magnetic Domain Evolution in Multiferroic Heterostructures. *J. Phys.: Condens. Matter* **2015**, *27*, 504005.

(2) Li, Z.; Hu, J.; Shu, L.; Zhang, Y.; Gao, Y.; Shen, Y.; Lin, Y.; Nan, C. W. A Simple Method for Direct Observation of the Converse Magnetoelectric Effect in Magnetic/Ferroelectric Composite Thin Films. *J. Appl. Phys.* **2011**, *110*, 096106.

(3) Mattheis, R.; Quednau, G. Determination of the Anisotropy Field Strength in Ultra-Thin Magnetic Films using Longitudinal MOKE and a Rotating. *J. Magn. Magn. Mater*. **1999,** *205*, 143.

(4) Zhang, S.; Zhao, Y. G.; Li, P. S.; Yang, J. J.; Rizwan, S.; Zhang, J. X.; Seidel, J.; Qu, T. L.; Yang, Y. J.; Luo, Z. L.; He, Q.; Zou, T.; Chen, Q. P.; Wang, J. W.; Yang, L. F.; Sun, Y.; Wu, Y. Z.; Xiao, X.; Jin, X. F.; Huang, J.; Gao, C.; Han, X. F.; Ramesh, R. Electric-Field Control of Nonvolatile Magnetization in $Co_{40}Fe_{40}B_{20}/Pb(Mg_{1/3}Nb_{2/3})_{0.7}Ti_{0.3}O_3$ Structure at Room Temperature. *Phys. Rev. Lett.* **2012**, *108*, 137203.

(5) Yang, L.; Zhao, Y.; Zhang, S.; Li, P.; Gao, Y.; Yang, Y.; Huang, H.; Miao, P.; Liu, Y.; Chen, A.; Nan, C. W.; Gao, C. Bipolar Loop-Like Non-Volatile Strain in the (001)-Oriented $Pb(Mg_{1/3}Nb_{2/3})O_3$-$PbTiO_3$ Single Crystals. *Sci. Rep.* **2014**, *4*, 4591.

(6) Lei, N.; Devolder, T.; Agnus, G.; Aubert, P.; Daniel, L.; Kim, J.; Zhao, W.; Trypiniotis, T.; Cowburn, R. P.; Chappert, C.; Ravelosona, D.; Lecoeur, P. Strain-Controlled Magnetic Domain Wall Propagation in Hybrid Piezoelectric/Ferromagnetic Structures. *Nat. Commun.* **2013**, *4*, 1378.